Tafolecimab mitigates ox-LDL-induced macrophage foam cell formation and inflammation by modulating SR-A/ABCG1 expression and inhibiting the NF-κB/MAPK pathways

XINYI YU[1,2], XIAODAN LIU[3], YUANYE DANG[4] and RUOXUAN LIU[1]

[1]Department of Pharmacy, The Affiliated Traditional Chinese Medicine Hospital, Guangzhou Medical University, Guangzhou, Guangdong 510645, P.R. China; [2]Guangzhou Municipal and Guangdong Provincial Key Laboratory of Molecular Target and Clinical Pharmacology, NMPA and State Key Laboratory of Respiratory Disease, School of Pharmaceutical Sciences, Guangzhou Medical University, Guangzhou, Guangdong 511436, P.R. China; [3]Guangzhou Institute of Pediatrics, Guangzhou Women and Children's Medical Center, Guangzhou Medical University, Guangdong Provincial Clinical Research Center for Child Health, Guangzhou, Guangdong 510623, P.R. China; [4]Key Laboratory of Molecular Target and Clinical Pharmacology, The Affiliated Traditional Chinese Medicine Hospital, NMPA and State Key Laboratory of Respiratory Diseases, School of Pharmaceutical Sciences, Guangzhou Medical University, Guangzhou, Guangdong 511436, P.R. China

Received December 30, 2025; Accepted July 9, 2026

DOI: 10.3892/br.2026.2189

Abstract. Macrophage foam-cell formation, triggered by excessive uptake of oxidized low-density lipoprotein (ox-LDL) and subsequent intracellular lipid accumulation, represents a critical pathological event in atherosclerotic plaque initiation that drives localized inflammatory responses. The present study investigated the effects of tafolecimab on ox-LDL-induced foam-cell formation and inflammatory responses in murine macrophages, and further explored the underlying molecular mechanisms. Foam-cell models were established by exposing RAW264.7 cells to 100 μg/ml ox-LDL for 24 h. The study groups included a blank control group, a model group, low-, medium- and high-dose tafolecimab groups (5, 10 and 20 μmol/l, respectively), and a positive control group treated with evolocumab. Intracellular lipid accumulation and cholesterol levels were evaluated using Oil Red O staining and a low-density lipoprotein-cholesterol (LDL-C) assay kit. Western blot analysis was performed to determine the expression of cholesterol metabolism-related proteins [class A scavenger receptor (SR-A) and ATP-binding cassette subfamily G member 1 (ABCG1)] and key components of the nuclear factor-κB (NF-κB)/mitogen-activated protein kinase (MAPK) signaling pathways (NF-κB p65 and phosphorylated p38). The concentrations of the inflammatory cytokines tumor necrosis factor-α (TNF-α) and interleukin-6 (IL-6) in the cell supernatant were quantified by enzyme-linked immunosorbent assay. Compared with the blank control, ox-LDL treatment markedly increased intracellular lipid-droplet accumulation and LDL-C content, confirming the successful establishment of a foam-cell model. *In vitro*, compared with the model group, tafolecimab reduced intracellular lipid accumulation and cholesterol content in a dose-dependent manner (P<0.001). In addition, tafolecimab significantly decreased the expression of the cholesterol influx receptor SR-A while increasing that of the cholesterol efflux transporter ABCG1 (P<0.001). Furthermore, it effectively inhibited the phosphorylation of NF-κB p65 and MAPK p38, which was accompanied by reduced secretion of TNF-α and IL-6 (P<0.001). The present results indicate that tafolecimab inhibits ox-LDL-induced macrophage foam-cell formation and inflammatory responses, likely by modulating the balance between SR-A-mediated cholesterol influx and ABCG1-mediated cholesterol efflux in favor of cholesterol efflux, and by inhibiting NF-κB and MAPK pathway activation.

Correspondence to: Dr Ruoxuan Liu, Department of Pharmacy, The Affiliated Traditional Chinese Medicine Hospital, Guangzhou Medical University, 95 Tiankun Third Road, Tianhe, Guangzhou, Guangdong 510645, P.R. China
E-mail: lrx1221@163.com

Key words: tafolecimab, atherosclerosis, macrophage foam cells, cholesterol metabolism, NF-κB signaling, MAPK signaling

Introduction

Atherosclerosis (AS) is the principal pathological basis of cardiovascular and cerebrovascular diseases, and is fundamentally a chronic inflammatory disorder. In particular, coronary artery disease remains a leading cause of mortality worldwide (1), accounting for ~1 in 4 mortalities, and is responsible for an estimated 17.8 million mortalities annually (1).

The development of AS typically is initiated by endothelial activation, followed by monocyte adhesion to the activated endothelium, transendothelial migration and subsequent differentiation into macrophages (2). Macrophages play a key role in the progression of AS. From a pathological perspective, macrophage-derived foam-cell formation follows a

well-defined sequence of events. During early AS, endothelial activation and dysfunction facilitate the subendothelial retention and modification of apolipoprotein B-containing lipoproteins, particularly low-density lipoprotein (LDL). Oxidized (ox)-LDL and other modified lipoproteins then promote the recruitment of circulating monocytes, which adhere to the activated endothelium, migrate into the intima and differentiate into macrophages. These macrophages take up large quantities of ox-LDL predominantly through scavenger receptors such as class A scavenger receptor (SR-A) and CD36, leading to progressive accumulation of cholesteryl ester in cytoplasmic lipid droplets and the generation of lipid-laden foam cells. Clusters of foam cells give rise to fatty streaks, the earliest detectable atherosclerotic lesions, which can subsequently develop into advanced plaques containing a necrotic core and thin fibrous cap in the setting of persistent lipid overload, chronic inflammatory activation and defective efferocytosis (2-4). From the initial lesion formation to the progression toward vulnerable plaques, accumulating evidence suggests that modulation of macrophage polarization can effectively influence disease progression (3). Macrophages internalize substantial levels of ox-LDL through the scavenger receptor SR-A, thereby promoting their transformation into lipid-laden foam cells, while the cholesterol transporter ATP-binding cassette subfamily G member 1 (ABCG1) mediates cholesterol efflux (4,5). Thus, maintenance of the balance between cholesterol influx and efflux is crucial for the development of targeted therapeutic strategies for AS.

Monoclonal antibodies directed against proprotein convertase subtilisin/kexin type 9 (PCSK9) have become an effective therapeutic option for lowering LDL-cholesterol (LDL-C) and reducing the risk of major adverse cardiovascular events (6). Among these agents, evolocumab is widely used in current clinical practice, and reduces LDL-C by ~60% at the end of the dosing interval, with a mean reduction of 65-68% maintained throughout the interval (7,8). Optical coherence tomography studies have demonstrated that, in patients with non-ST-segment elevation myocardial infarction (NSTEMI), the addition of evolocumab to background statin therapy significantly improves the compositional characteristics of coronary plaques. Compared with the placebo group, patients treated with evolocumab exhibited a greater increase in minimum fibrous cap thickness (+42.7 μm vs. +21.5 μm; P=0.015), along with significant reductions in maximum lipid arc and macrophage index (P=0.04). Furthermore, in lipid-rich plaque regions, evolocumab showed a more pronounced trend toward plaque stabilization, and intravascular ultrasound (IVUS) assessment revealed a greater reduction in percent atheroma volume (-2.29% vs. -0.61%; P=0.009). These findings suggest that the addition of evolocumab to statin therapy following acute coronary syndrome promotes coronary plaque stabilization and regression, supporting a mechanistic basis for reducing future cardiovascular events through favorable modification of plaque composition (9). Tafolecimab (SINTBILO®) is a subcutaneously administered monoclonal antibody targeting PCSK9 that was developed by Innovent Biologics (Suzhou) Co., Ltd. and was approved in China in 2023 for adults with primary hyperlipidemia, including heterozygous familial hypercholesterolaemia and non-familial hypercholesterolemia, or with mixed dyslipidemia whose LDL-C remains above target despite moderate- or high-intensity statin therapy. Although tafolecimab markedly lowers LDL-C, total cholesterol and apolipoprotein B, it remains unclear whether it also exerts direct anti-foam-cell and anti-inflammatory effects on macrophages residing within the vascular wall beyond its systemic lipid-lowering effects (10).

In the present study, *in vitro* experiments were conducted using an ox-LDL-induced foam-cell model in RAW264.7 macrophages. In total, two control groups, namely a blank control group and a model control group, together with six experimental groups treated with low, medium or high doses of tafolecimab or evolocumab were established. Intracellular lipid accumulation was assessed by Oil Red O staining and LDL-C assay. Western blot analysis was performed to evaluate changes in the expression of key proteins involved in cholesterol metabolism, including SR-A and ABCG1, as well as the phosphorylation status of components of the nuclear factor-κB (NF-κB)/mitogen-activated protein kinase (MAPK) signaling pathway, including NF-κB p65 and phosphorylated (p)-p38. The secretion levels of the inflammatory cytokines tumor necrosis factor-α (TNF-α) and interleukin-6 (IL-6) were measured by enzyme-linked immunosorbent assay (ELISA). The present study aimed to systematically elucidate the effects of tafolecimab on macrophage foam-cell formation and inflammation, investigate the underlying molecular mechanisms with a focus on cholesterol metabolism and related signaling pathways, and perform a parallel comparison with evolocumab to provide a stronger experimental and theoretical basis for the clinical application of tafolecimab.

Materials and methods

Cell line, reagents and instruments. The murine monocyte-macrophage cell line RAW264.7 was obtained from iCell. Tafolecimab and evolocumab were supplied by Innovent Biologics, Inc. Ox-LDL was purchased from Yiyuan Biotechnologies (cat. no. YB-002). The Oil Red O staining kit was purchased from Sigma-Aldrich; Merck KGaA (cat. no. O0625-25g). The LDL-C and total cholesterol assay kits (cat. nos. A113-1-1 and A111-1-1, respectively) were obtained from Nanjing Jiancheng Bioengineering Institute. Primary antibodies against SR-A (cat. no. 17858-1-AP), ABCG1 (cat. no. 13578-1-AP), p38 (cat. no. 14064-1-AP), p-p38 (cat. no. 28796-1-AP), NF-κB p65 (cat, no. 10745-1-AP), p-NF-κB p65 (cat.no.82335-1-RR), vinculin (cat.no.26520-1-AP), tubulin (cat. no. 66031-1-Ig) and GAPDH (cat. no. 10494-1-AP) were purchased from Proteintech Group, Inc., and goat anti-rabbit mouse igG-HRP (cat. no. M21003) was obtained from Abmart. The enhanced chemiluminescence (ECL) detection kit was provided by Shanghai Yeasen Biotechnology Co., Ltd. (cat. no. 36222ES60). TNF-α and IL-6 ELISA kits were obtained from Uping Bio; Hangzhou Zhenyoupin Biotechnology Co., Ltd. (cat. nos. SYP-M0036 and SYP-M0031, respectively). CO_2 incubators, microplate readers, and western blot electrophoresis and transfer systems were provided by the Institute of Pediatrics, Women and Children's Medical Center, Guangzhou Medical University (Guangzhou, China).

Cell culture and treatment groups. RAW264.7 cells were subjected to mycoplasma testing and short tandem repeat

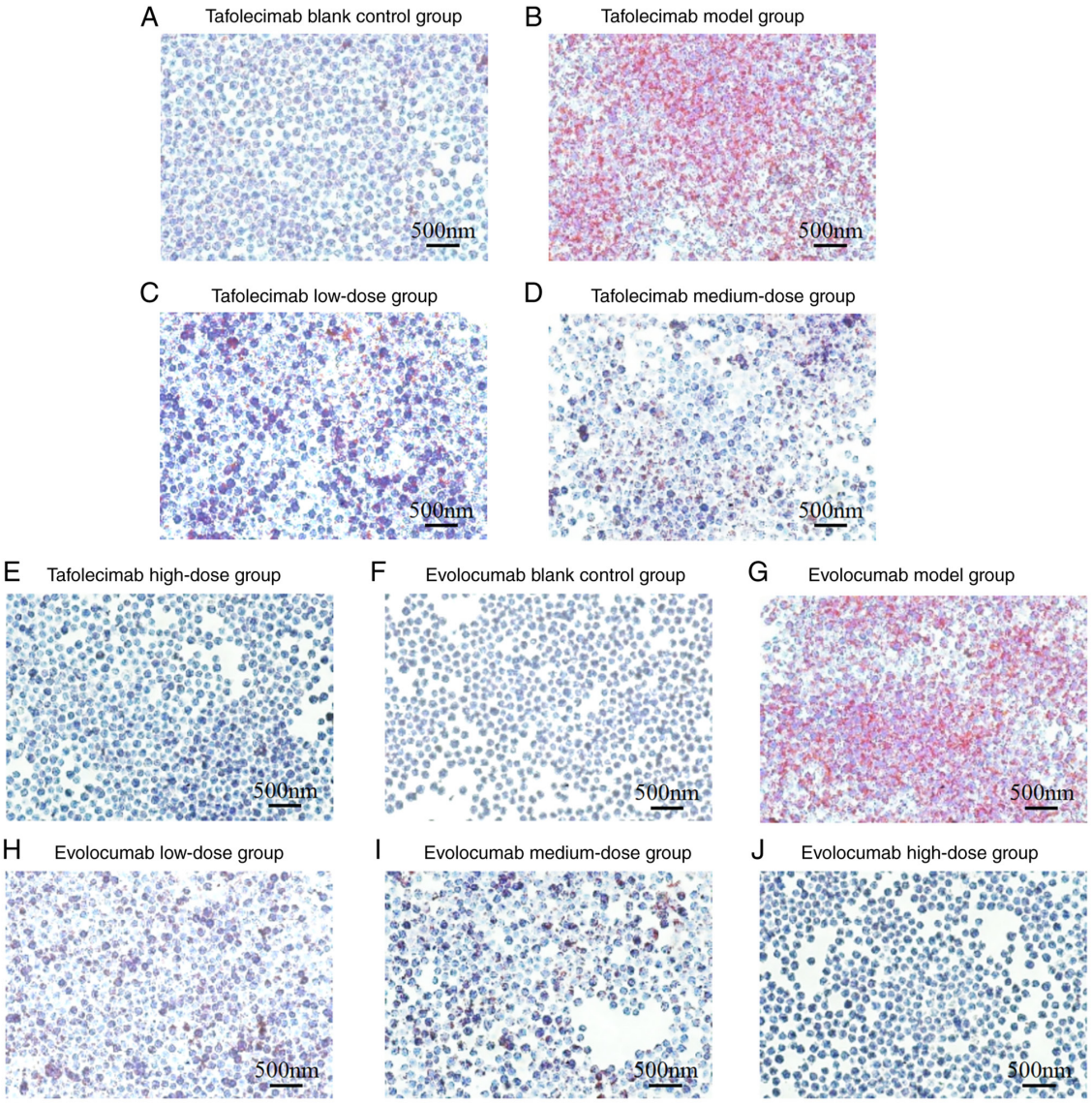

Figure 1. Oil Red O staining of cells treated with different drug concentrations. (A-E) Tafolecimab treatment groups. (F-J) Evolocumab treatment groups. The groups received the following designated treatments: (A and F) Blank control group; (B and G) model groups; (C) tafolecimab low-dose group; (H) evolocumab low-dose group; (D) tafolecimab medium-dose group; (I) evolocumab medium-dose group; (E) tafolecimab high-dose group; and (J) evolocumab high-dose group.

profiling. RAW264.7 cells were maintained in DMEM supplemented with 10% fetal bovine serum (BIOEXPLORER®; Guangzhou Yufeng Biotechnology Co., Ltd.) at 37˚C in a humidified with 5% CO_2. The experimental design comprised a blank control group, a model group, and tafolecimab or evolocumab treatment groups. In the blank control group, cells were cultured under standard conditions. In the model group, cells were cultured in serum-free medium for 24 h, followed by exposure to 100 μg/ml ox-LDL for 24 h. For the tafolecimab groups, cells were first cultured in serum-free medium for 24 h and then pretreated with tafolecimab at 5, 10 or 20 μmol/l for 24 h. Subsequently, 100 μg/ml ox-LDL was added without removing the drug-containing medium, and the cells were co-incubated with tafolecimab and ox-LDL for a further 24 h. The evolocumab groups were treated using the same protocol. The concentrations of tafolecimab and evolocumab (5, 10 and 20 μmol/l) were selected based on preliminary dose-finding experiments in RAW264.7 cells (11,12), which showed robust, concentration-dependent effects on foam-cell formation in the absence of detectable cytotoxicity. Although these concentrations fall within the order of magnitude of free antibody levels that may be achievable in patients receiving therapeutic doses, they were selected primarily for exploratory mechanistic studies rather than for establishing direct clinical equivalence.

Oil Red O staining. Cells were seeded into 24-well plates at a density of $3x10^6$ cells per well and treated according to their corresponding experimental group. After treatment, the cells were washed with PBS, fixed with 4% paraformaldehyde for 20 min at room temperature. After fixation, cells were washed three times with PBS. Oil Red O stock solution was prepared by dissolving 0.25 g Oil Red O powder in 50 ml isopropanol and stored away from light. The working solution was mixed with the stock solution and distilled water at a volume ratio of 3:2 and filtered before use. Cells were incubated with the working solution at room temperature in the dark for 20 min.

After discarding the staining solution, each well was rinsed with 60% isopropanol for 30 sec. Following removal of the 60% isopropanol solution, hematoxylin was added for 1 min for counterstaining. Foam-cell formation was assessed by light microscopy on the basis of red intracellular lipid-droplet accumulation, and representative images were acquired. Quantitative analysis of Oil Red O-positive lipid droplets was conducted using ImageJ software (version 1.54u7; National Institutes of Health).

Measurement of intracellular cholesterol content. Cells were seeded into 6-well plates at a density of $1x10^6$ cells per well, and after the designated treatments, were harvested. The prepared cell suspension was collected and centrifuged at 165 x g for 10 min at 25˚C, after which the supernatant was discarded and the cell pellet was retained. The pellet was washed twice with PBS, followed by centrifugation at 165 x g for 10 min at 25˚C, the supernatant was then removed again to reserve the cell pellet. Cells were lysed with 2% Triton X-100 (Glpbio Technology) on ice for 40 min. The lysate was directly subjected to detection without centrifugation. After incubation at 37˚C for 10 min, the absorbance of each well was measured at a wavelength of 500 nm. Statistical analysis was performed using GraphPad Prism version 10.1.2 (Dotmatics).

Western blot analysis of protein expression. Following the corresponding assigned treatments, cells were washed with ice-cold PBS and lysed in RIPA lysis buffer (Thermo Fisher Scientific, Inc.), supplemented with 1% protease and phosphatase inhibitors on ice for 30 min. The lysates were then centrifuged at 12,000 x g for 15 min at 4˚C to collect the supernatant. Total cellular protein concentration was quantified using a BCA protein assay kit (Thermo Fisher Scientific, Inc.). Equal amounts of total cellular protein (10 μg per lane) were separated by 10% SDS-PAGE electrophoresis and subsequently electrotransferred onto PVDF membranes. Membranes were blocked with 5% non-fat milk at room temperature for 1 h, and then the membranes were incubated with primary antibodies against SR-A, ABCG1, NF-κB p65, p-p65, p38, p-p38, vinculin, tubulin and GAPDH, followed by HRP-conjugated secondary antibodies. All primary antibodies were diluted at 1:2,000 and incubated with membranes overnight at 4˚C. The corresponding HRP-conjugated secondary antibodies were diluted at 1:5,000 and incubated for 1 h at room temperature. Immunoreactive bands were visualized using ECL, and band intensities were quantified using ImageJ software (version 1.54u7). Target protein expression was normalized to the appropriate loading controls GAPDH, tubulin and vinculin.

ELISA for detecting inflammatory cytokines. Cell culture supernatants were collected, and the concentrations of TNF-α and IL-6 were quantified using ELISA kits according to the manufacturer's instructions.

Statistical analysis. All data were analyzed using GraphPad Prism (version 10.1.2; Dotmatics) and are presented as the mean ± standard deviation. Comparisons among multiple groups were performed using one-way analysis of variance (ANOVA), followed by Dunnett's post hoc test for pairwise comparisons against the control group (model). P<0.05 was considered to indicate a statistically significant difference. All experiments were performed with three independent biological replicates.

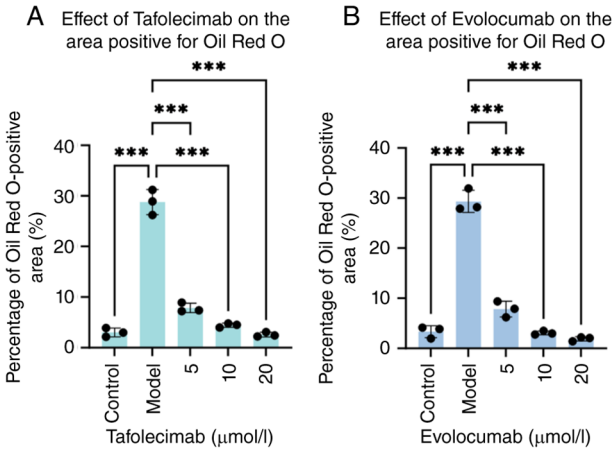

Figure 2. Assessment of the therapeutic effects of tafolecimab and evolocumab in an atherosclerosis model. Effects of tafolecimab and evolocumab on lipid accumulation in ox-LDL-treated macrophages. (A) Percentage of Oil Red O-positive areas in macrophages treated with increasing concentrations of tafolecimab. (B) Percentage of Oil Red O-positive areas in macrophages treated with increasing concentrations of evolocumab. Experimental groups included blank control (Control), ox-LDL model (Model), and drug-treated groups with low (5 μmol/l), medium (10 μmol/l) and high (20 μmol/l) concentrations. Data are presented as the mean ± standard deviation from three independent experiments. One-way analysis of variance followed by Dunnett's post hoc test was used for statistical analysis. ***P<0.001 vs. the model group. Ox-LDL, oxidized low-density lipoprotein.

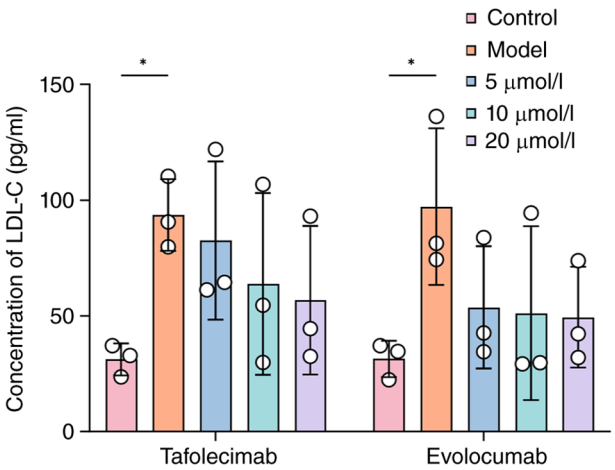

Figure 3. Effects of tafolecimab and evolocumab on intracellular LDL-C levels in ox-LDL-treated macrophages. LDL-C concentrations in macrophages treated with increasing doses of tafolecimab. LDL-C concentrations in macrophages treated with increasing doses of evolocumab. Experimental groups included a blank control (Control), ox-LDL model (Model), and drug-treated groups at low (5 μmol/l), medium (10 μmol/l) and high (20 μmol/l) doses. Data are presented as the mean ± standard deviation (n=3). One-way analysis of variance followed by Dunnett's post hoc test was used for statistical analysis. *P<0.05 vs. the model group. LDL-C, low-density lipoprotein cholesterol; ox-LDL, oxidized low-density lipoprotein.

Results

Tafolecimab inhibits macrophage foam cell formation. Oil Red O staining revealed that cells in the blank control

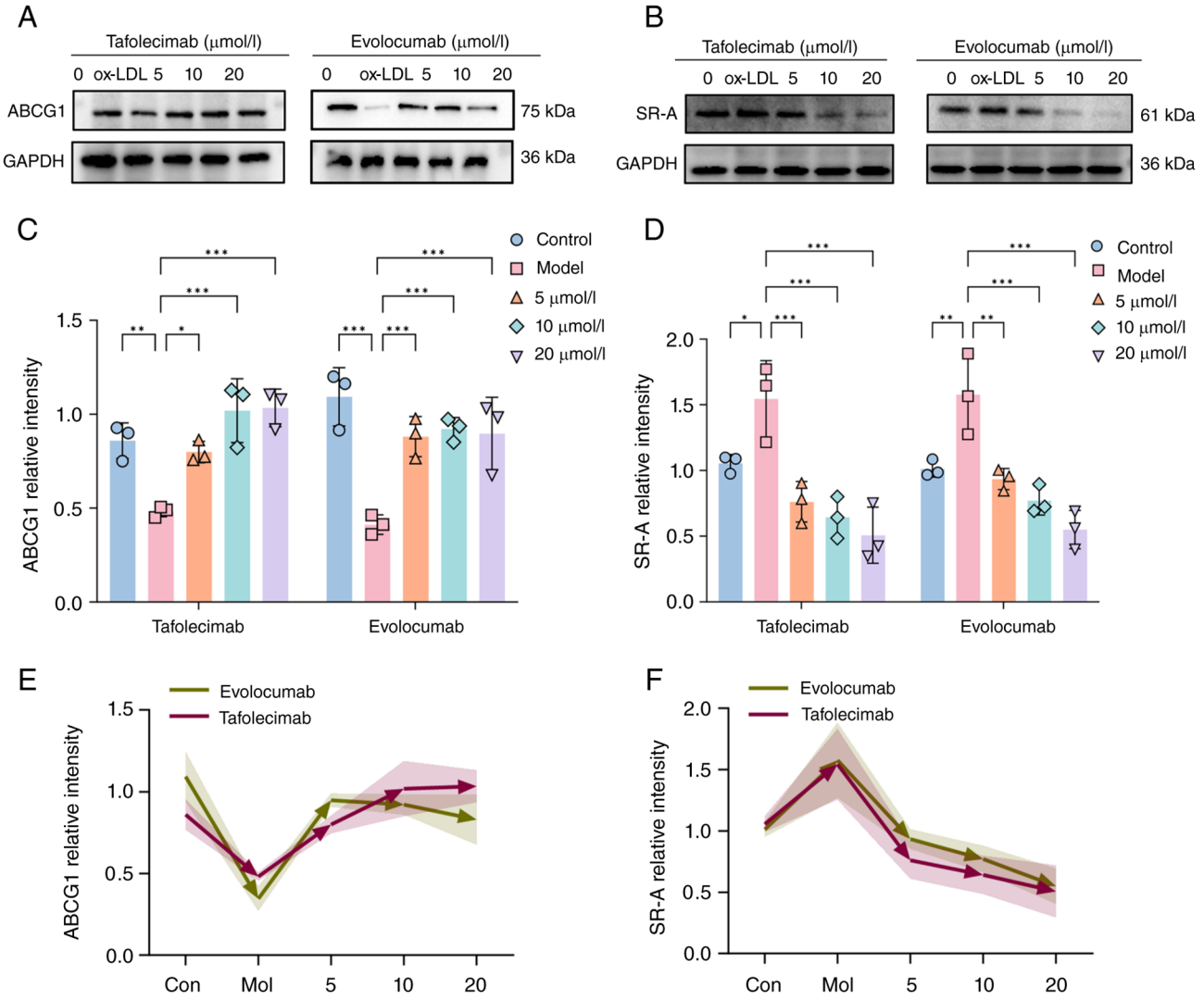

Figure 4. Effects of tafolecimab and evolocumab on ABCG1 and SR-A protein expression in ox-LDL-stimulated macrophages. (A and B) Representative western blot images showing (A) ABCG1 and (B) SR-A protein levels in macrophages treated with ox-LDL in the absence or presence of tafolecimab or evolocumab (5, 10, and 20 μmol/l). GAPDH was used as a loading control. Molecular weights are indicated on the right. (C and D) Quantitative analysis of (A) ABCG1 and (B) SR-A protein expression normalized to GAPDH and expressed as the relative intensity compared with the model group. (E and F) Trend analysis of (E) ABCG1 and (F) SR-A relative protein density across treatment groups. Data are presented as the mean ± standard deviation from three independent experiments. Statistical significance was determined by one-way ANOVA followed by Dunnett's post hoc test. *P<0.05, **P<0.01 and ***P<0.001. ABCG1, ATP-binding cassette subfamily G member 1; SR-A, class A scavenger receptor; ox-LDL, oxidized low-density lipoprotein; Con, control; Mol, ox-LDL model group.

group retained normal morphology and showed no evident red intracellular lipid droplets, whereas cells in the model group exhibited marked cytoplasmic lipid-droplet accumulation, indicative of foam-cell formation. Relative to the model group, all tafolecimab pretreatment markedly reduced intracellular lipid-droplet accumulation in a dose-dependent manner (Figs. 1A-E and 2A). Comparable inhibitory effects were observed in the evolocumab-treated groups (Figs. 1F-J and 2B).

Tafolecimab reduces intracellular cholesterol accumulation. The findings of the LDL-C assay were consistent with those obtained by Oil Red O staining. Cellular LDL-C levels were markedly increased in the model group relative to the blank control (P<0.05). Tafolecimab reduced intracellular LDL-C content in a dose-dependent manner (Fig. 3), and the extent of this reduction was comparable to that observed with evolocumab, suggesting that both agents exert similar inhibitory effects on intracellular LDL-C accumulation (Fig. 3).

Tafolecimab regulates the expression of cholesterol-metabolism-related proteins. As shown in Fig. 4, ox-LDL markedly altered the expression of key regulators of cholesterol influx and efflux in RAW264.7 macrophages. Relative to the blank control group, ox-LDL stimulation significantly reduced ABCG1 expression (P<0.01) and increased SR-A expression (P<0.05), which is consistent with a shift toward a cholesterol-accumulating phenotype.

Pretreatment with tafolecimab for 24 h, followed by co-incubation with ox-LDL, significantly and dose-dependently upregulated ABCG1 and downregulated SR-A relative to the ox-LDL model group (P<0.05 for all concentrations; Fig. 4C and D). Evolocumab produced a highly similar pattern

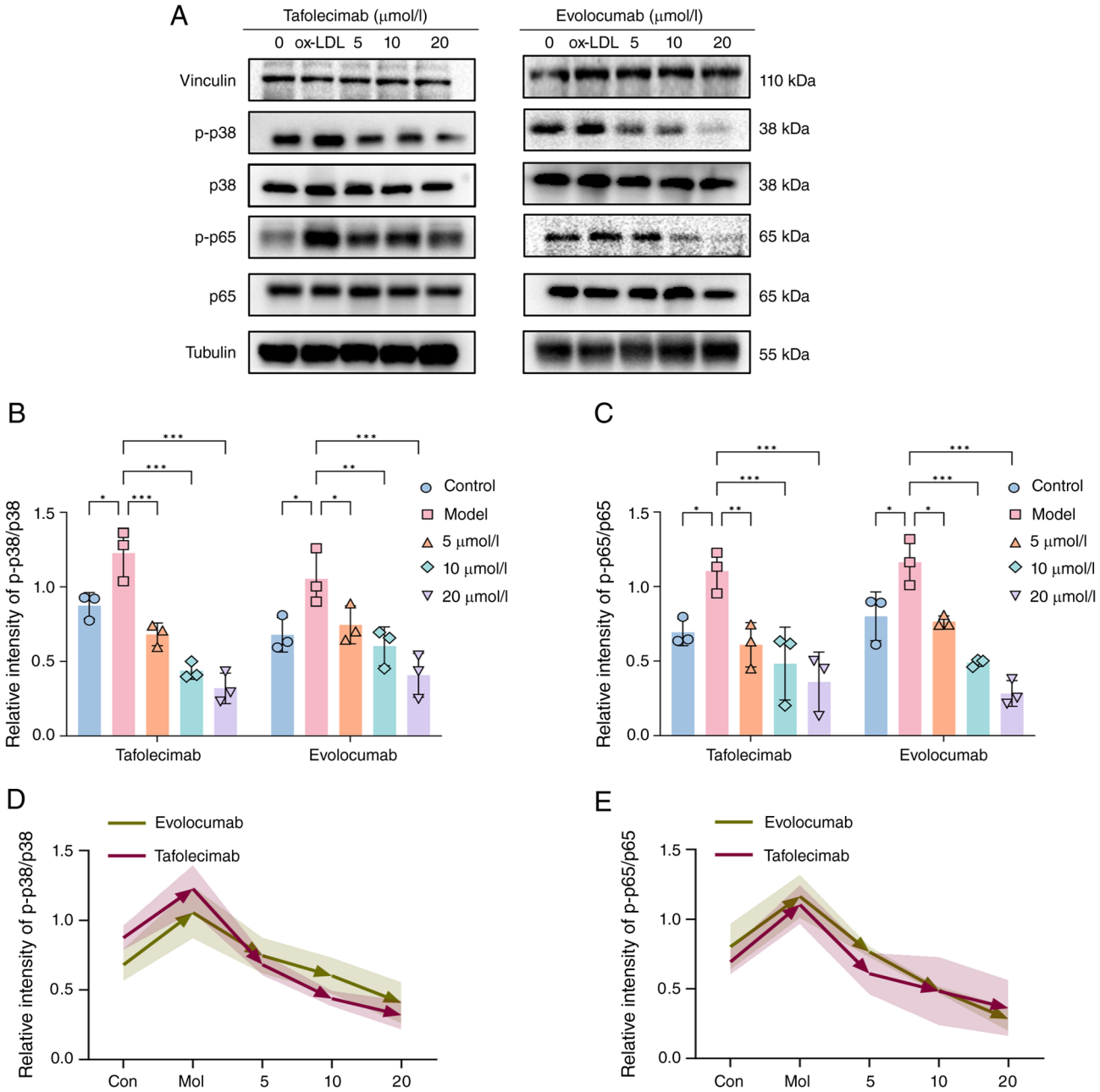

Figure 5. Effects of tafolecimab and evolocumab on p38 and p65 phosphorylation in ox-LDL-stimulated macrophages. (A) Representative western blot images showing the protein expression levels of p-p38, total p38, p-p65, and total p65 in macrophages stimulated with ox-LDL and treated with tafolecimab or evolocumab at indicated concentrations (5, 10, and 20 μmol/l). Vinculin and tubulin were used as loading controls. Molecular weights are indicated on the right. (B and C) Quantitative analysis of (B) p-p38 (B) and (C) p-p65 protein levels, normalized to their respective total proteins (p38 or p65) and expressed as relative intensity compared with the model group. (D and E) Trend analysis of relative (D) p-p38 and (E) p-p65 protein expression across treatment groups. Data are presented as the mean ± standard deviation from three independent experiments. Statistical analysis was performed using one-way ANOVA followed Dunnett's post hoc test. *P<0.05, **P<0.01 and ***P<0.001. ox-LDL, oxidized low-density lipoprotein; p-p38, phosphorylated p38; p-p65, phosphorylated p65; Con, control group; Mol, ox-LDL model group.

of regulation, and the magnitude of its effects was comparable to that of tafolecimab across the tested concentrations (Fig. 4E and F). These findings suggest that both PCSK9 inhibitors promote a cholesterol-efflux-favouring profile in ox-LDL-treated macrophages through coordinated modulation of ABCG1 and SR-A expression.

Tafolecimab suppresses the activation of the NF-κB and MAPK signaling pathway. To further investigate the underlying mechanisms, the activation status of key signaling pathways was assessed. Ox-LDL markedly increased the phosphorylation of MAPK p38 and NF-κB p65. By contrast, pretreatment with tafolecimab suppressed the phosphorylation of these proteins, which is consistent with inhibition of NF-κB and MAPK signaling. Similarly, evolocumab also reduced the phosphorylation levels of p38 and p65 (Fig. 5).

Tafolecimab inhibits the secretion of inflammatory cytokines. ELISA demonstrated that IL-6 and TNF-α (Fig. 6) levels in the culture supernatant were significantly elevated in the

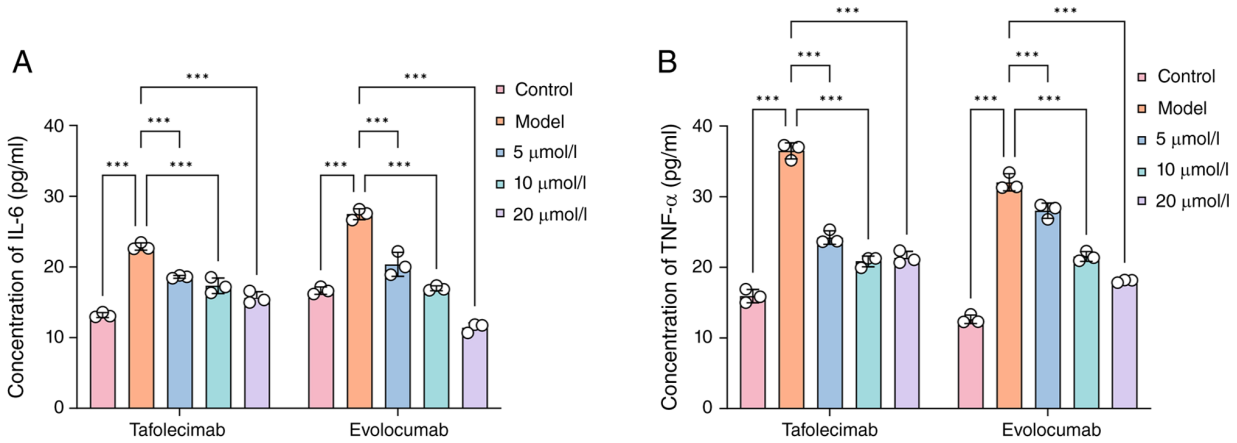

Figure 6. Inhibitory effects of tafolecimab on the secretion of the inflammatory cytokines TNF-α and IL-6. (A and B) Cytokine levels in the cell supernatant were measured using ELISA. (A) IL-6 concentration. (B) TNF-α concentration. Experimental groups included low-, medium- and high-dose tafolecimab and evolocumab groups. Blank control and model groups were included for reference. Compared with the blank control group, TNF-α and IL-6 levels in the model group were significantly elevated (P<0.001). Tafolecimab treatment dose-dependently suppressed the secretion of both cytokines (P<0.001). Data are presented as the mean ± standard deviation (n=3). One-way analysis of variance followed by Dunnett's post hoc test was used for statistical analysis. ***P<0.001 vs. the model group.

model group relative to the blank control group (P<0.001). Tafolecimab markedly reduced the secretion of both cytokines in a dose-dependent manner (P<0.001). As the positive control, evolocumab also significantly downregulated the expression of IL-6 and TNF-α (P<0.001).

Discussion

AS is a leading cause of global morbidity and mortality, driving the pathogenesis of disabling peripheral artery disease, stroke and myocardial infarction (13). Since its identification in the early 2000s, PCSK9 has emerged as a central regulator of cholesterol homeostasis, and its favorable pharmacological profile has underscored its immense therapeutic potential in the context of AS (14). The present study provides the first systematic demonstration of the pleiotropic mechanisms by which tafolecimab attenuates macrophage foam-cell formation and mitigates inflammatory responses. Mechanistically, it was found that tafolecimab promotes a more favorable state of cholesterol homeostasis by concurrently suppressing SR-A-mediated cholesterol influx and enhancing ABCG1-mediated cholesterol efflux, thereby shifting macrophages toward a cholesterol-efflux-promoting phenotype (14-18). Together with ATP-binding cassette subfamily A member 1 (ABCA1), ABCG1 is a key ATP-binding cassette transporter that facilitates cholesterol efflux from macrophages to HDL and other extracellular acceptors. By limiting the accumulation of free and esterified cholesterol, ABCG1 has a central role in preserving intracellular cholesterol homeostasis and restraining foam-cell formation (17). The tafolecimab-induced upregulation of ABCG1 observed in the present study may thereby contribute not only to reduced intracellular cholesterol burden, but also to the reprogramming of macrophages towards an anti-atherogenic, inflammation-resolving state (17,18). Notably, the present study further delineated the upstream signaling pathways induced by the molecular targets of tafolecimab. The NF-κB and MAPK signaling pathways serve as core regulators of inflammation and cellular stress responses (19-23). Activation of NF-κB and MAPK signaling in lesional macrophages has profound consequences for plaque biology. NF-κB-driven transcription amplifies the production of pro-inflammatory cytokines, including TNF-α and IL-6, which not only sustain local inflammation but also impair endothelial nitric oxide bioavailability, thereby exacerbating endothelial dysfunction and promoting a pro-thrombotic, vasoconstrictive microenvironment. MAPK signaling also plays a central role in regulating macrophage survival, proliferation and the expression of matrix-degrading enzymes, processes that can compromise fibrous-cap integrity. Sustained activation of these pathways favors macrophage apoptosis and secondary necrosis in the lipid core, expansion of the necrotic core and thinning of the fibrous cap, ultimately increasing the risk of plaque rupture and thrombosis. Therefore, the ability of tafolecimab to attenuate NF-κB and MAPK activation and to reduce TNF-α and IL-6 secretion in ox-LDL-treated macrophages may, in principle, translate into improved endothelial function, reduced necrotic core formation and enhanced plaque stability *in vivo* (24).

Tafolecimab is a fully human monoclonal antibody that neutralizes circulating PCSK9 within the extracellular compartment. Canonically, PCSK9 binds to LDL receptors (LDLR) and targets them for lysosomal degradation, thereby increasing circulating LDL-C levels. In macrophages, however, PCSK9 appears to exert a function that extends beyond LDLR reregulation. Previous experimental evidence indicates that PCSK9 is expressed by macrophages and can influence scavenger receptors, including SR-A, cholesterol efflux transporters and pro-inflammatory signaling pathways (25,26).

In this context, the effects of tafolecimab observed in the present study are likely to be multifactorial. By neutralizing PCSK9, tafolecimab may alter LDLR-dependent lipoprotein uptake and intracellular cholesterol handling, while also indirectly modulating SR-A and ABCG1 expression through changes in cellular cholesterol burden and membrane composition. In parallel, PCSK9 inhibition may directly suppress PCSK9-driven pro-inflammatory signaling,

thereby decreasing NF-κB/MAPK activation and downstream cytokine release. Defining the relative contributions of LDLR-dependent and -independent pathways will require future studies incorporating PCSK9 knockdown or knockout models and receptor-specific interventions.

In the present study, evolocumab was included as an established comparator PCSK9 inhibitor. At equivalent concentrations *in vitro*, tafolecimab and evolocumab exerted broadly similar effects on foam-cell formation, cholesterol handling and inflammatory signaling, indicating that the observed responses are likely to be largely class-related. However, individual PCSK9 monoclonal antibodies recognize distinct epitopes and may differ in binding affinity, pharmacokinetic behaviour and tissue distribution *in vivo*. In principle, such differences could give rise to subtle qualitative or quantitative variations in the modulation of PCSK9-LDLR interactions, as well as in other PCSK9-dependent effects on vascular cells. Since the present *in vitro* system does not enable rigorous pharmacokinetic or epitope-specific comparisons, further structural and *in vivo* studies will be required to establish whether tafolecimab confers any advantages beyond its LDL-C-lowering efficacy. Several limitations should be considered when interpreting the present findings. First, all experiments were conducted in a single murine macrophage-like cell line (RAW264.7). Although RAW264.7 cells are widely used in atherosclerosis research, immortalized cell lines cannot fully capture the phenotypic heterogeneity and functional complexity of primary human monocyte-derived macrophages or distinct lesional macrophage subsets. Validation in primary macrophages and *in vivo* models of atherosclerosis will therefore be essential. The current analyses focused on SR-A and ABCG1 as representative mediators of cholesterol influx and efflux, respectively, and on the NF-κB and MAPK signaling pathways as central inflammatory pathways. However, foam-cell formation and vascular inflammation are governed by a broader network of receptors, transporters and signaling cascades, including CD36, LOX-1, ABCA1, JNK, ERK and inflammasome-related pathways components, which were not examined in the present study. Additionally, the present study was limited to relatively short-term (24 h) treatments and did not address the long-term effects of tafolecimab on macrophage survival, apoptosis, efferocytosis or necrotic core formation, all of which are major determinants of plaque stability. Therefore, future studies in animal models and human tissues will be needed to establish whether the acute cellular effects observed *in vitro* translate into sustained alteration in plaque burden, plaque composition and clinical outcomes. These findings suggest that tafolecimab may benefit high-risk patients with residual inflammatory risk who continue to experience cardiovascular events despite achieving target LDL-C levels. If validated *in vivo*, tafolecimab could offer a dual benefit by addressing both lipid and inflammatory risks to enhance plaque stability.

In summary, tafolecimab was shown to effectively attenuate ox-LDL-induced macrophage foam-cell formation and inflammatory responses. Mechanistically, tafolecimab ameliorated ox-LDL alteration in cholesterol homeostasis by modulating the expression of key cholesterol influx and efflux, while concurrently suppressing NF-κB and MAPK inflammatory signaling. Collectively, these findings provide mechanistic insights into the anti-atherogenic effects of tafolecimab and support its potential as a therapeutic strategy for AS.

Acknowledgements

Not applicable.

Funding

The present study was supported by the Xinhuo Inheritance Special Scientific Research Fund (grant no. XHXC017), the Hunan Provincial Natural Science Foundation (University Joint Fund Project; grant no. 2025JJ90126), and the Special Research Project of National Health Commission Capacity Building and Continuing Education Center (grant no. GWJJZX20251007036), which enabled the completion of key experiments in the present study.

Availability of data and materials

The data generated in the present study may be requested from the corresponding author.

Authors' contributions

RL conceived the study, designed the overall experimental protocol, led project planning and funding acquisition, and was responsible for the final review and approval of the manuscript. XY conducted the *in vitro* experiments, performed systematic data integration and processing, and drafted and revised the manuscript. XL made substantial contributions to the conception and design of the study, and critically reviewed the manuscript for important intellectual content. YD made substantial contributions to the acquisition of experimental data, as well as the formal analysis and interpretation of data. RL and XY confirm the authenticity of all the raw data. All authors read and approved the final manuscript.

Ethics approval and consent to participate

Not applicable.

Patient consent for publication

Not applicable.

Competing interests

The authors declare that they have no competing interests.

References

1. Kawai K, Finn AV and Virmani R; Subclinical Atherosclerosis Collaborative: Subclinical atherosclerosis: Part 1: What is it? Can it be defined at the histological level? Arterioscler Thromb Vasc Biol 44: 12-23, 2024.
2. Koelwyn GJ, Corr EM, Erbay E and Moore KJ: Regulation of macrophage immunometabolism in atherosclerosis. Nat Immunol 19: 526-537, 2018.
3. Wu J, He S, Song Z, Chen S, Lin X, Sun H, Zhou P, Peng Q, Du S, Zheng S and Liu X: Macrophage polarization states in atherosclerosis. Front Immunol 14: 1185587, 2023.

4. Ma C, Li Y, Tian M, Deng Q, Qin X, Lu H, Gao J, Chen M, Weinstein LS, Zhang M, *et al*: Gsα regulates macrophage foam cell formation during atherosclerosis. Circ Res 134: e34-e51, 2024.
5. Kunjathoor VV, Febbraio M, Podrez EA, Moore KJ, Andersson L, Koehn S, Rhee JS, Silverstein R, Hoff HF and Freeman MW: Scavenger receptors class A-I/II and CD36 are the principal receptors responsible for the uptake of modified low density lipoprotein leading to lipid loading in macrophages. J Biol Chem 277: 49982-49988, 2002.
6. O'Donoghue ML, Giugliano RP, Wiviott SD, Atar D, Keech A, Kuder JF, Im K, Murphy SA, Flores-Arredondo JH, López JAG, *et al*: Long-term evolocumab in patients with established atherosclerotic cardiovascular disease. Circulation 146: 1109-1119, 2022.
7. Grundy SM, Stone NJ, Bailey AL, Beam C, Birtcher KK, Blumenthal RS, Braun LT, de Ferranti S, Faiella-Tommasino J, Forman DE, *et al*: 2018 AHA/ACC/AACVPR/AAPA/ABC/ACPM/ADA/AGS/APhA/ASPC/NLA/PCNA guideline on the management of blood cholesterol: Executive summary: A report of the American college of cardiology/American heart association task force on clinical practice guidelines. Circulation 139: e1046-e1081, 2019.
8. Mach F, Baigent C, Catapano AL, Koskinas KC, Casula M, Badimon L, Chapman MJ, De Backer GG, Delgado V, Ference BA, *et al*: 2019 ESC/EAS guidelines for the management of dyslipidaemias: Lipid modification to reduce cardiovascular risk. Eur Heart J 41: 111-188, 2020.
9. Nicholls SJ, Kataoka Y, Nissen SE, Prati F, Windecker S, Puri R, Hucko T, Aradi D, Herrman JPR, Hermanides RS, *et al*: Effect of evolocumab on coronary plaque phenotype and burden in statin-treated patients following myocardial infarction. JACC Cardiovasc Imaging 15: 1308-1321, 2022.
10. Keam SJ: Tafolecimab: First approval. Drugs 83: 1545-1549, 2023.
11. White HD, Steg PG and Schwartz GG: Myocardial infarction and evolocumab. JAMA Cardiol 6: 1220-1221, 2021.
12. Sabatine MS, Giugliano RP, Keech AC, Honarpour N, Wiviott SD, Murphy SA, Kuder JF, Wang H, Liu T, Wasserman SM, *et al*: Evolocumab and clinical outcomes in patients with cardiovascular disease. N Engl J Med 376: 1713-1722, 2017.
13. Lu L, Sun X, Qin Y and Guo X: The signaling pathways involved in the antiatherosclerotic effects produced by Chinese herbal medicines. BioMed Res Int 2018: 5392375, 2018.
14. Hummelgaard S, Vilstrup JP, Gustafsen C, Glerup S and Weyer K: Targeting PCSK9 to tackle cardiovascular disease. Pharmacol Ther 249: 108480, 2023.
15. Liu X, Zheng T, Zhang Y, Zhao Y, Liu F, Dai S, Zhang M, Zhang W, Zhang C, Zhang M and Li X: Endothelial dickkopf-1 promotes smooth muscle cell-derived foam cell formation via USP53-mediated deubiquitination of SR-A during atherosclerosis. Int J Biol Sci 20: 2943-2964, 2024.
16. Cheng W, Shu M, Kuang L, Bai X, Jia X, Zhao Y, Lu Y, Zhu L, Wang L, Zhu Y, *et al*: Scavenger receptor a mediates glycated LDL transcytosis across endothelial cells to promote atherosclerosis. Int J Biol Macromol 235: 123836, 2023.
17. Zheng S, Huang H, Li Y, Wang Y, Zheng Y, Liang J, Zhang S, Liu M and Fang Z: Yin-xing-tong-mai decoction attenuates atherosclerosis via activating PPARγ-LXRα-ABCA1/ABCG1 pathway. Pharmacol Res 169: 105639, 2021.
18. Wang H, Yang Y, Sun X, Tian F, Guo S, Wang W, Tian Z, Jin H, Zhang Z and Tian Y: Sonodynamic therapy-induced foam cells apoptosis activates the phagocytic PPARγ-LXRα-ABCA1/ABCG1 pathway and promotes cholesterol efflux in advanced plaque. Theranostics 8: 4969-4984, 2018.
19. Frambach SJCM, de Haas R, Smeitink JAM, Rongen GA, Russel FGM and Schirris TJJ: Brothers in arms: ABCA1- and ABCG1-mediated cholesterol efflux as promising targets in cardiovascular disease treatment. Pharmacol Rev 72: 152-190, 2020.
20. Zhang S, Xu P, Zhu Z, Zhou L, Li J, Zhou R, Kan Y, Li Y, Yu X, Zhao J, *et al*: Acetylation of $p65^{Lys310}$ by p300 in macrophages mediates anti-inflammatory property of berberine. Redox Biol 62: 102704, 2023.
21. Mao H, Zhao X and Sun SC: NF-κB in inflammation and cancer. Cell Mol Immunol 22: 811-839, 2025.
22. Kaszycki J and Kim M: Epigenetic regulation of transcription factors involved in NLRP3 inflammasome and NF-kB signaling pathways. Front Immunol 16: 1529756, 2025.
23. Chu C, Ru H, Chen Y, Xu J, Wang C and Jin Y: Gallic acid attenuates LPS-induced inflammation in Caco-2 cells by suppressing the activation of the NF-κB/MAPK signaling pathway. Acta Biochim Biophys Sin (Shanghai) 56: 905-915, 2024.
24. Kambhampati V, Eedara A and Andugulapati SB: Yohimbine treatment improves pulmonary fibrosis by attenuating the inflammation and oxidative stress via modulating the MAPK pathway. Biochem Pharmacol 230: 116613, 2024.
25. Seidah NG and Prat A: The multifaceted biology of PCSK9. Endocr Rev 43: 558-582, 2022.
26. Peng Z, Lv SJ, Chen H, Rao H, Guo Z, Wan Q, Yang J, Zhang Y, Liu DP, Chen HZ and Wang M: Disruption of PCSK9 suppresses inflammation and attenuates abdominal aortic aneurysm formation. Arterioscler Thromb Vasc Biol 45: e1-e14, 2025.